

Multi[2]rotaxanes with Gold
Nanoparticles as Centers

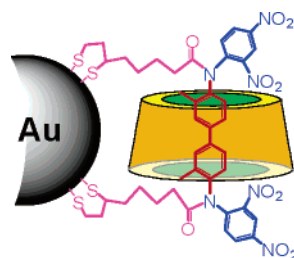
Yan-Li Zhao, Yong Chen, Min Wang, and Yu Liu*

Department of Chemistry, State Key Laboratory of Elemento-Organic Chemistry,
Nankai University, Tianjin 300071, P. R. China

yuliu@nankai.edu.cn

Received December 8, 2005

ABSTRACT



The multi[2]rotaxanes with gold nanoparticles as centers are constructed by introducing chromophoric β -cyclodextrin-based [2]rotaxanes on the surface of gold nanoparticles, which show good photophysical and electrochemical properties superior to the parent rotaxane.

Noble metal and semiconductor nanoparticles are of current interest for their application in a wide variety of areas including catalysis, optoelectronic and magnetic nanodevices, chemical sensors, nanotechnology, and biological sciences.¹ Among these particles, the gold nanoparticles constitute a very active topic of research in chemistry.^{2,3} Various organic and biological molecules, such as sulfur-based compounds,^{4,5}

proteins,⁶ DNA,^{7,8} enzymes,⁹ and cyclodextrins,^{10,11} are used to functionalize the gold nanoparticles. Among them, cyclodextrins (CDs) have attracted the extensive interests of scientists because of their high solubilization ability, low toxicity, and specific recognition ability toward many model

(1) (a) Alivisatos, A. P. *Science* **1996**, *271*, 933–937. (b) Elghanian, R.; Storhoff, J. J.; Mucic, R. C.; Letsinger, R. L.; Mirkin, C. A. *Science* **1997**, *277*, 1078–1081. (c) Chen, S.; Ingram, R. S.; Hostetler, M. J.; Pietron, J. J.; Murray, R. W.; Schaaff, T. G.; Khoury, J. T.; Alvarez, M. M.; Whetten, R. L. *Science* **1998**, *280*, 2098–2101. (d) Quake, S. R.; Scherer, A. *Science* **2000**, *290*, 1536–1540. (e) van Delden, R. A.; ter Wiel, M. K. J.; Pollard, M. M.; Vicario, J.; Koumura, N.; Feringa, B. L. *Nature* **2005**, *437*, 1337–1340.

(2) Niemeyer, C. M. *Angew. Chem., Int. Ed.* **2001**, *40*, 4128–4158.

(3) (a) Daniel, M.-C.; Astruc, D. *Chem. Rev.* **2004**, *104*, 293–346. (b) Burda, C.; Chen, X.; Narayanan, R.; El-Sayed, M. A. *Chem. Rev.* **2005**, *105*, 1025–1102. (c) Love, J. C.; Estroff, L. A.; Kriebel, J. K.; Nuzzo, R. G.; Whitesides, G. M. *Chem. Rev.* **2005**, *105*, 1103–1169. (d) Rosi, N. L.; Mirkin, C. A. *Chem. Rev.* **2005**, *105*, 1547–1562. (e) Crooks, R. M.; Zhao, M.; Sun, L.; Chechik, V.; Yeung, L. K. *Acc. Chem. Res.* **2001**, *34*, 181–190. (f) Thomas, K. G.; Kamat, P. V. *Acc. Chem. Res.* **2003**, *36*, 888–898. (g) Shenhar, R.; Rotello, V. M. *Acc. Chem. Res.* **2003**, *36*, 549–561.

(4) (a) Fitzmaurice, D.; Rao, S. N.; Preece, J. A.; Stoddart, J. F.; Wenger, S.; Zaccheroni, N. *Angew. Chem., Int. Ed.* **1999**, *38*, 1147–1150. (b) Schroedter, A.; Weller, H. *Angew. Chem., Int. Ed.* **2002**, *41*, 3218–3221. (c) Kang, Y.; Taton, T. A. *Angew. Chem., Int. Ed.* **2005**, *44*, 409–412. (d) Tshikhudo, T. R.; Demuru, D.; Wang, Z.; Brust, M.; Secchi, A.; Arduini, A.; Pochini, A. *Angew. Chem., Int. Ed.* **2005**, *44*, 2913–2916.

(5) (a) Hasobe, T.; Imahori, H.; Kamat, P. V.; Ahn, T. K.; Kim, S. K.; Kim, D.; Fujimoto, A.; Hirakawa, T.; Fukuzumi, S. *J. Am. Chem. Soc.* **2005**, *127*, 1216–1228. (b) Fresco, Z. M.; Fréchet, J. M. J. *J. Am. Chem. Soc.* **2005**, *127*, 8302–8303. (c) Abad, J. M.; Mertens, S. F. L.; Pita, M.; Fernández, V. M.; Schiffrin, D. J. *J. Am. Chem. Soc.* **2005**, *127*, 5689–5694. (d) Maye, M. M.; Lim, I.-M. S.; Luo, J.; Rab, Z.; Rabinovich, D.; Liu, T.; Zhong, C.-J. *J. Am. Chem. Soc.* **2005**, *127*, 1519–1529. (e) Raehm, L.; Hamann, C.; Kern, J.-M.; Sauvage, J.-P. *Org. Lett.* **2000**, *2*, 1991–1994. (f) Kell, A. J.; Stringle, D. L. B.; Workentin, M. S. *Org. Lett.* **2000**, *2*, 3381–3384.

(6) (a) Chan, W. C. W.; Nie, S. *Science* **1998**, *281*, 2016–2018. (b) Maxwell, D. J.; Taylor, J. R.; Nie, S. *J. Am. Chem. Soc.* **2002**, *124*, 9606–9612. (c) Mattoussi, H.; Mauro, J. M.; Goldman, E. R.; Anderson, G. P.; Sundar, V. C.; Mikulec, F. V.; Bawendi, M. G. *J. Am. Chem. Soc.* **2000**, *122*, 12142–12150. (d) Clapp, A. R.; Medintz, I. L.; Mauro, J. M.; Fisher, B. R.; Bawendi, M. G.; Mattoussi, H. *J. Am. Chem. Soc.* **2004**, *126*, 301–310. (e) You, C.-C.; De, M.; Rotello, V. M. *Org. Lett.* **2005**, *7*, 5685–5688.

(7) (a) Tkachenko, A. G.; Xie, H.; Coleman, D.; Glomm, W.; Ryan, J.; Anderson, M. F.; Franzen, S.; Feldheim, D. L. *J. Am. Chem. Soc.* **2003**, *125*, 4700–4701. (b) Sato, K.; Hosokawa, K.; Maeda, M. *J. Am. Chem. Soc.* **2003**, *125*, 8102–8103. (c) Liu, J.; Lu, Y. *J. Am. Chem. Soc.* **2004**, *126*, 12298–12305. (d) Storhoff, J. J.; Lazarides, A. A.; Mucic, R. C.; Mirkin, C. A.; Letsinger, R. L.; Schatz, G. C. *J. Am. Chem. Soc.* **2000**, *122*, 4640–4650. (e) Jin, R.; Wu, G.; Li, Z.; Mirkin, C. A.; Schatz, G. C. *J. Am. Chem. Soc.* **2003**, *125*, 1643–1654.

substrates. For example, Matsui,^{10b} Kaifer,^{10c-e} and Reinhoudt^{10f-i} et al. have separately reported the preparation and aggregation of thioCD-modified gold nanoparticles and their applications in the phase transfer, catalysis, and molecular printboard. On the other hand, rotaxanes and polyrotaxanes constructed by the inclusion complexation of host CDs and guest molecules have attracted more and more attention because of their potential to serve as molecular devices, molecular machines, and functional materials.^{12,13} Therefore, one can expect that the combination of rotaxanes/polyrotaxanes and gold nanoparticles will reveal many significant functions and thus open a new and interesting research access in the fields of life and material science. However, the CD rotaxane-modified gold nanoparticles have rarely been reported so far, to the best of our knowledge.^{10e,11} In the present work, we successfully prepared a rotaxane-capped gold nanoparticle by introducing chromophoric [2]rotaxanes on the surface of gold nanoparticles (Figure 1), and the resulting gold nanoparticle could show some good photophysical and electrochemical properties.

The rotaxane-capped gold nanoparticle **4** is prepared according to the procedure shown in Figure 1. First, the [2]-pseudorotaxane **2** is obtained by the reaction of β -CD/o-tolidine inclusion complex **1**¹⁴ with 2,4-dinitrofluorobenzene. A microcalorimetric titration experiment at 25 °C in an

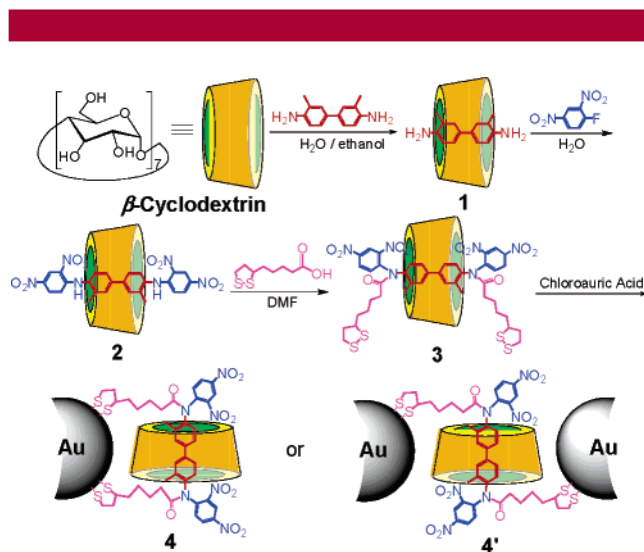


Figure 1. Synthesis of rotaxane-capped gold nanoparticle **4**.

aqueous buffer solution (pH 7.2) gives the stability constant of **1** as $8866 \pm 257 \text{ M}^{-1}$, indicating a satisfactory stability of **1**, which will favor its further reaction with 2,4-dinitrofluorobenzene. Besides the FT-IR, ¹H NMR, and elemental analysis data, the formation of **1** and **2** can be also verified by the 2D ROESY spectra, which show the clear NOE correlations between the aromatic protons in **1** or **2** and the interior protons of CD cavity. Second, the [2]-pseudorotaxane **2** is converted into the [2]rotaxane **3** in a relatively low yield (18%) after reaction with lipic acids. Finally, the reaction of **3** with chloroauric acid (HAuCl₄) in the presence of NaBH₄ gives **4** in 53% yield (the weight of **4** obtained)/(the sum of the weight of HAuCl₄ and **3** used). In this step, the soluble gold precursor (HAuCl₄) is reduced to form metallic gold nuclei, and then the adsorption of disulfides onto the surface of gold nuclei breaks the S–S bonds in **3** to produce the rotaxane-capped gold nanoparticle through the formation of S–Au bond. Owing to the polarity of many hydroxyl groups in the β -CD units, which afford a polar character to the surface of gold nanoparticle,^{10d} **4** displays a moderate water solubility up to 0.80 mg·mL⁻¹ and can remain dissolved without any apparent aggregation or precipitation for several weeks.

Some spectral and microscopic data give the useful information about the structure of rotaxane-capped gold nanoparticle **4**. The UV spectrum of parent gold nanoparticle¹⁵ shows a characteristic band at 520 nm in aqueous solution for the surface plasmon resonance (SPR) absorption of gold. However, in the UV spectrum of **4**, this SPR band red shifts to 529 nm. Moreover, a absorption maximum at 281 nm assigned to the [2]rotaxane moiety is also observed in the UV spectrum of **4**. In addition, the ¹H NMR spectrum of **4** in D₂O also displays the characteristic signals of the corresponding protons in **3**, especially the characteristic signals of

(8) (a) Deng, Z.; Tian, Y.; Lee, S.-H.; Ribbe, A. E.; Mao, C. *Angew. Chem., Int. Ed.* **2005**, *44*, 3582–3585. (b) Park, S.-J.; Lazarides, A. A.; Mirkin, C. A.; Brazis, P. W.; Kannewurf, C. R.; Letsinger, R. L. *Angew. Chem., Int. Ed.* **2000**, *39*, 3845–3848. (c) Niemeyer, C. M.; Ceyhan, B.; Hazarika, P. *Angew. Chem., Int. Ed.* **2003**, *42*, 5766–5770. (d) Hazarika, P.; Ceyhan, B.; Niemeyer, C. M. *Angew. Chem., Int. Ed.* **2004**, *43*, 6469–6471.

(9) (a) Kanaras, A. G.; Wang, Z.; Bates, A. D.; Cosstick, R.; Brust, M. *Angew. Chem., Int. Ed.* **2003**, *42*, 191–194. (b) Pardo-Yissar, V.; Katz, E.; Wasserman, J.; Willner, I. *J. Am. Chem. Soc.* **2003**, *125*, 622–623. (c) Liu, J.; Khitrov, G. A.; Vergona, D. E.; Reich, N. O.; Strouse, G. F. *J. Am. Chem. Soc.* **2002**, *124*, 7644–7645. (d) Peña, S. R. N.; Raina, S.; Goodrich, G. P.; Fedoroff, N. V.; Keating, C. D. *J. Am. Chem. Soc.* **2002**, *124*, 7314–7323.

(10) (a) Sylvestre, J.-P.; Kabashin, A. V.; Sacher, E.; Meunier, M.; Luong, J. H. T. *J. Am. Chem. Soc.* **2004**, *126*, 7176–7177. (b) Banerjee, I. A.; Yu, L.; Matsui, H. *J. Am. Chem. Soc.* **2003**, *125*, 9542–9543. (c) Liu, J.; Alvarez, J.; Ong, W.; Román, E.; Kaifer, A. E. *J. Am. Chem. Soc.* **2001**, *123*, 11148–11154. (d) Liu, J.; Alvarez, J.; Ong, W.; Kaifer, A. E. *Nano Lett.* **2001**, *1*, 57–60. (e) Liu, J.; Xu, R.; Kaifer, A. E. *Langmuir* **1998**, *14*, 7337–7339. (f) Crespo-Biel, O.; Dordi, B.; Reinhoudt, D. N.; Huskens, J. *J. Am. Chem. Soc.* **2005**, *127*, 7594–7600. (g) Huskens, J.; Deij, M. A.; Reinhoudt, D. N. *Angew. Chem., Int. Ed.* **2002**, *41*, 4467–4471. (h) de Jong, M. R.; Huskens, J.; Reinhoudt, D. N. *Chem. Eur. J.* **2001**, *7*, 4164–4170. (i) Nijhuis, C. A.; Huskens, J.; Reinhoudt, D. N. *J. Am. Chem. Soc.* **2004**, *126*, 12266–12267.

(11) (a) Liu, Y.; Zhao, Y.-L.; Chen, Y.; Wang, M. *Macromol. Rapid Commun.* **2005**, *26*, 401–406. (b) Liu, Y.; Wang, H.; Chen, Y.; Ke, C.-F.; Liu, M. *J. Am. Chem. Soc.* **2005**, *127*, 657–666.

(12) (a) Nepogodiev, S. A.; Stoddart, J. F. *Chem. Rev.* **1998**, *98*, 1959–1976. (b) Raymo, F. M.; Stoddart, J. F. *Chem. Rev.* **1999**, *99*, 1643–1663. (c) Harada, A. *Acc. Chem. Res.* **2001**, *34*, 456–464. (d) Okada, M.; Harada, A. *Org. Lett.* **2004**, *6*, 361–364. (e) Kawaguchi, Y.; Harada, A. *J. Am. Chem. Soc.* **2000**, *122*, 3797–3798. (f) Taylor, P. N.; O’Connell, M. J.; McNeill, L. A.; Hall, M. J.; Aplin, R. T.; Anderson, H. L. *Angew. Chem., Int. Ed.* **2000**, *39*, 3456–3460. (g) Onagi, H.; Carrozzini, B.; Cascarano, G. L.; Easton, C. J.; Edwards, A. J.; Lincoln, S. F.; Rae, A. D. *Chem. Eur. J.* **2003**, *9*, 5971–5977. (h) Onagi, H.; Blake, C. J.; Easton, C. J.; Lincoln, S. F. *Chem. Eur. J.* **2003**, *9*, 5978–5988. (i) Wang, Q.-C.; Qu, D.-H.; Ren, J.; Chen, K.; Tian, H. *Angew. Chem., Int. Ed.* **2004**, *43*, 2661–2665. (j) Qu, D.-H.; Wang, Q.-C.; Ren, J.; Tian, H. *Org. Lett.* **2004**, *6*, 2085–2088.

(13) (a) Liu, Y.; Zhao, Y.-L.; Zhang, H.-Y.; Song, H.-B. *Angew. Chem., Int. Ed.* **2003**, *42*, 3260–3263. (b) Liu, Y.; You, C.-C.; Zhang, H.-Y.; Kang, S.-Z.; Zhu, C.-F.; Wang, C. *Nano Lett.* **2001**, *1*, 613–616. (c) Liu, Y.; Li, L.; Fan, Z.; Zhang, H.-Y.; Wu, X.; Liu, S.-X.; Guan, X.-D. *Nano Lett.* **2002**, *2*, 257–261.

(14) Liu, Y.; Zhao, Y.-L.; Zhang, H.-Y.; Li, X.-Y.; Liang, P.; Zhang, X.-Z.; Xu, J.-J. *Macromolecules* **2004**, *37*, 6362–6369.

(15) Grabar, K. C.; Freeman, R. G.; Hommer, M. B.; Natan, M. J. *Anal. Chem.* **1995**, *67*, 735–743.

the aromatic protons, lipic carboxylate protons, and CD backbone protons (C1-H, C2-H, C3-H, C4-H, C5-H, C6-H), but the signals for the nanoparticle-immobilized CDs are broadened as compared with those in the ^1H NMR spectrum of **3**. This phenomenon is similar to that reported by Kaifer and co-workers,^{10c} and the fast relaxation and environmental heterogeneities are thought to be responsible for these line-broadening effects. Furthermore, the results of elemental analysis experiments show that the ratios among C, H, N, and S in **4** are mostly consistent with those in **3**, which indicates the presences of **3** in the nanoparticles **4**. A comparison of the FT-IR spectra of rotaxane-capped gold nanoparticle **4** with its precursors (parent gold nanoparticle, lipoic acid, and compounds **1–3**) indicates that the FT-IR spectrum of **4** is obviously different from that of parent gold nanoparticle but resembles that of **3**. No S–H stretching band at ca. 2560 cm^{-1} can be observed in the IR spectrum of **4**, showing that the most of disulfide moieties are absorbed on the surface of gold, because the unreacted disulfide moieties of lipoic acids will be reduced to the S–H bonds in the presence of NaBH_4 . Furthermore, four characteristic reflections around $2\theta = 38.1^\circ$ ($d = 2.35\text{ \AA}$), 44.4 (2.03), 64.7 (1.45), and 77.6 (1.23), which correspond to the (111), (200), (220), and (311) planes of the cubic phase of Au, in the XRD diffractogram of parent gold nanoparticle appreciably shift to ca. $2\theta = 38.5^\circ$ ($d = 2.33\text{ \AA}$), 45.4 (1.99), 66.3 (1.41), and 75.3 (1.26) in the diffractogram of **4**. Moreover, the reflections around $2\theta = 18.7^\circ$ ($d = 4.75\text{ \AA}$) and 28.4 (3.14) in the diffractogram of parent gold nanoparticle disappear after gold nanoparticles are reacted with **3**, and two new reflections around $2\theta = 27.3^\circ$ ($d = 3.26\text{ \AA}$) and 31.7 (2.82) appear in the diffractogram of **4**. Therefore, these phenomena jointly indicate the adsorption of **3** on the surface of gold nanoparticle through the conversion of the S–S bond in **3** to the S–Au bond.¹⁶ In addition, the average size of the gold nanoparticle **4** can be determined from the width of reflection in the powder X-ray diffraction (XRD) pattern according to the Scherrer formula $D = 0.9\lambda/(\beta \cos \theta)$, where β is the full width at the half-maximum of peak, θ is the angle of diffraction, and λ is the wavelength of X-ray radiation.¹⁷ The resultant value of D calculated from the (111) reflection ($2\theta = 38.5^\circ$, $d = 2.33\text{ \AA}$) of the cubic phase of Au in **4** is ca. 4.0 nm .

By assuming the core shape of nanoparticle to be spherical and the nanoparticles with a uniform size, the average number (N) of rotaxane units around one nanoparticle and the average surface area (Ψ) occupied by one rotaxane unit can be calculated by the following equation (also see the Supporting Information)

$$\Psi = S_{\text{Au}}/N$$

where S_{Au} is the surface area of the gold nanoparticle. N is

(16) (a) Wen, X. R.; Linton, W.; Formaggio, F.; Toniolo, C.; Samulski, E. T. *J. Phys. Chem. A* **2004**, *108*, 9673–9681. (b) Miura, Y.; Kimura, S.; Imanishi, Y.; Umemura, J. *Langmuir* **1998**, *14*, 6935–6940. (c) Willey, T. M.; Vance, A. L.; Bostedt, C.; van Buuren, T.; Meulenberg, R. W.; Terminello, L. J.; Fadley, C. S. *Langmuir* **2004**, *20*, 4939–4944.

(17) (a) Zhang, P.; Li, J.; Liu, D.; Qin, Y.; Guo, Z.-X.; Zhu, D. *Langmuir* **2004**, *20*, 1466–1472. (b) Leff, D. V.; Ohara, P. C.; Heath, J. R.; Gelbart, W. M. *J. Phys. Chem.* **1995**, *99*, 7036–7041.

the number of rotaxane units on each gold nanoparticle, and Ψ is the average surface area occupied by one rotaxane unit. According to the elemental analysis, TG-DTA, and ICP-MS results (the proportion of gold in **4**: ca. 13% by ICP-MS, ca. 17% by elemental analysis, ca. 12% by TG-DTA), the average number of rotaxane units around one nanoparticle is calculated to be 8, and the average surface area occupied by one rotaxane unit is 2.8 nm^2 .

Transmission electron microscopy (TEM) provides the direct information about the shape, size, and size distribution of rotaxane-capped gold nanoparticles. As shown in Figure 2, a typical TEM image of **4** shows numerous discrete gold

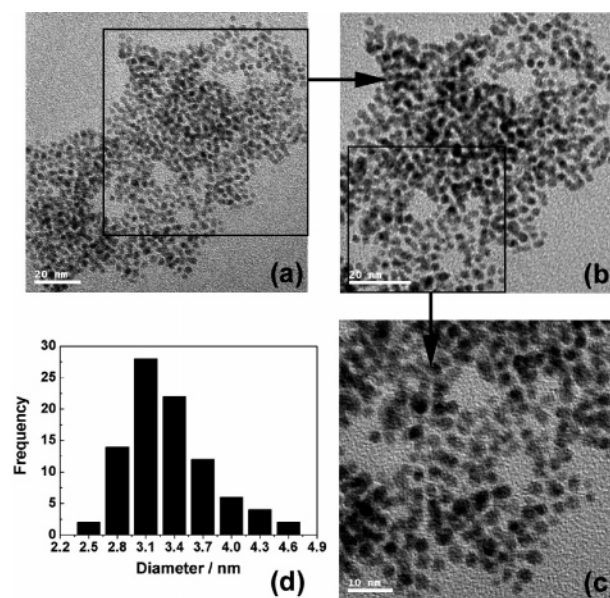


Figure 2. (a–c) Typical TEM images of **4**. The size labels are 20 nm for (a) and (b) 10 nm for (c). (d) Size-dependent histogram of **4**. Some large TEM images are shown in the Supporting Information.

nanoparticles with an average diameter of $3.5 \pm 1.1\text{ nm}$, which is in good agreement with the XRD results. Furthermore, the aggregation of nanoparticle are also observed in the TEM images, which may be attributed to the multivalent adsorption of **3** on the surfaces of gold nanoparticles. (**4'** in Figure 1). Interestingly, the size range of parent gold nanoparticles is $30\text{–}50\text{ nm}$ determined by TEM, which is larger than that of nanoparticle **4**. This phenomenon indicates that the introduction of cyclodextrin rotaxanes can change the size and distribution of gold nanoparticles, which is consistent with the reported results.^{10a,18}

Significantly, the gold nanoparticle **4** exhibits some exciting photophysical and electrochemical behaviors. In the control experiment, the gold nanoparticle without rotaxane cap is nonfluorescent, and the emission spectrum of **1** shows

(18) (a) Liu, Y.; Male, K. B.; Bouvrette, P.; Luong, J. H. T. *Chem. Mater.* **2003**, *15*, 4172–4180. (b) Kabashin, A. V.; Meunier, M.; Kingston, C.; Luong, J. H. T. *J. Phys. Chem. B* **2003**, *107*, 4527–4531.

a maximum at 406.0 nm with an excitation wavelength of 290.0 nm, while **3** displays two maxima at 391 and 550 nm with an excitation wavelength of 330.0 nm. It is well-known that the gold nanoparticles have an effect of quenching the fluorescence.¹⁹ After introducing the rotaxane units to the gold nanoparticle, the resultant gold nanoparticle **4** only exhibits a fluorescent emission band at 417 nm under the excitation at 290 nm, which indicates that the gold nanoparticle partially quenches the fluorescence of rotaxane **3**. This phenomenon may suggest the presence of charge-transfer process from chromophores in the rotaxanes to gold nanoparticles during the fluorescence experiments.¹⁹ Moreover, the cyclic voltammogram (CV) experiments (Figure 3) in a DMF solution of $[\text{N}(\text{C}_4\text{H}_9)_4]\text{PF}_6$ shows that the rotaxane-capped gold nanoparticle **4** gives an electrochemical active cycle in the potential range between ca. -1.7 V and ca. $+1.0$ V. The electrochemical reduction curve of **4** shows a strong peak at E (anodic potential) = 0.67 V. In the control experiments, the parent gold nanoparticle displays an almost electrochemical inactive cycle, while the electrochemical reduction curve of either **2** or **3** gives two CV signals at ca. -1.2 V and -1.5 V. The strong CV signals of **4** indicates that **4** has a satisfactory electron-accepting ability, which may be attributed to the efficient charge transfer from the chromophores in the rotaxanes to the gold nanoparticles in **4**.²⁰ In addition, the repeated scanning gives almost the same curve (e.g., in the fifth scanning), revealing that **4** is electrochemically stable.

In conclusion, we succeed in achieving an organization of CD-based rotaxane around gold nanoparticles through the

(19) (a) Lee, W. I.; Bae, Y.; Bard, A. J. *J. Am. Chem. Soc.* **2004**, *126*, 8358–8359. (b) Oh, E.; Hong, M.-Y.; Lee, D.; Nam, S.-H.; Yoon, H. C.; Kim, H.-S. *J. Am. Chem. Soc.* **2005**, *127*, 3270–3271. (c) You, C.-C.; De, M.; Han, G.; Rotello, V. M. *J. Am. Chem. Soc.* **2005**, *127*, 12873–12881.

(20) (a) Labande, A.; Ruiz, J.; Astruc, D. *J. Am. Chem. Soc.* **2002**, *124*, 1782–1789. (b) Daniel, M.-C.; Ruiz, J.; Nlate, S.; Blais, J.-C.; Astruc, D. *J. Am. Chem. Soc.* **2003**, *125*, 2617–2628. (c) Boulas, P. L.; Gómez-Kaifer, M.; Echegoyen, L. *Angew. Chem., Int. Ed.* **1998**, *37*, 216–247.

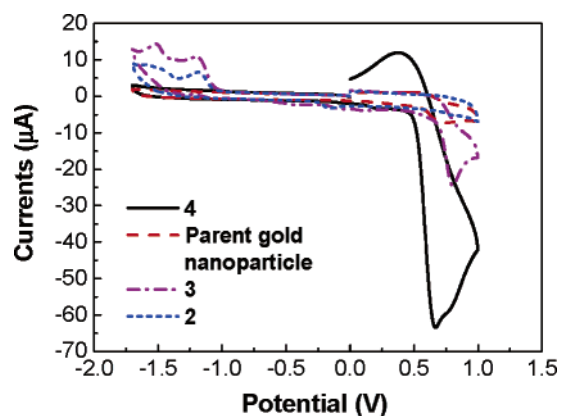


Figure 3. Cyclic voltammograms of **2–4** and parent gold nanoparticle in DMF solutions containing $[\text{N}(\text{C}_4\text{H}_9)_4]\text{PF}_6$.

association of rotaxane with gold particles, and this rotaxane-capped gold nanoparticle exhibits good photophysical and electrochemical properties. Benefiting from the fascinating functions of gold nanoparticles and rotaxanes, this kind of water-soluble inorganic–organic hybrid material will find future applications in many fields of chemistry and biology.

Acknowledgment. We thank NNSFC (Nos. 90306009, 20402008, 20421202, and 20572052) for the financial support. We also thank the reviewers for their highly valuable suggestions regarding the revision.

Supporting Information Available: Experimental details and corresponding spectra. This material is available free of charge via the Internet at <http://pubs.acs.org>.

OL052978C